

Supporting Information

Hollow Mesoporous Ruthenium Nanoparticles Conjugated Bispecific Antibody for Targeted Anti-Colorectal Cancer Response of Combination Therapy

Meng Xu,^{a,‡} Yayu Wen,^{a,‡} Yanan Liu,^{a,*} Xianjie Tan,^a Xu Chen,^a Xufeng Zhu,^a Chunfang
Wei,^a Lanmei Chen,^{b,*} Zhong Wang,^c Jie Liu,^{a,*}

^a Department of Chemistry, College of Chemistry and Materials Science, Jinan University,
Guangzhou 510632, China.

^b Dongguan Key Laboratory of Drug Design and Formulation Technology, School of
Pharmacy, Guangdong Medical University, Dongguan 523808, China.

^c Center for Cellular & Structural Biology, School of Pharmaceutical Sciences, Sun Yat-Sen
University, Guangzhou 510632, China.

* Corresponding authors: Lanmei Chen, E-mail: lanmeichen@126.com. Yanan Liu, E-mail:
yananliu0321@163.com. Jie Liu, E-mail: tliuliu@jnu.edu.cn.

‡ These authors contributed equally.

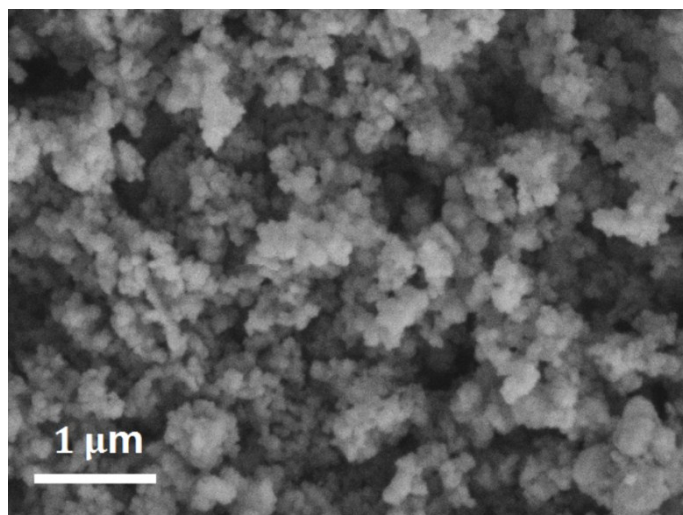
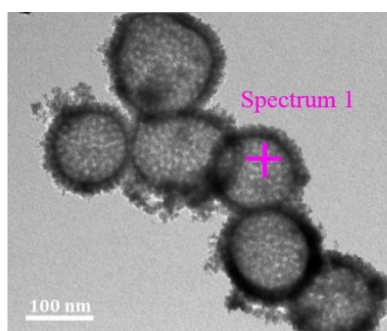


Fig. S1 Low-resolution SEM of hollow mesoporous Ru particles. Scale bars, 1 μm .



Element	Weight%	Atomic%
C	6.81	32.05
O	1.94	6.85
Cu	30.50	27.12
Ru	60.75	33.97
Totals	100.00	

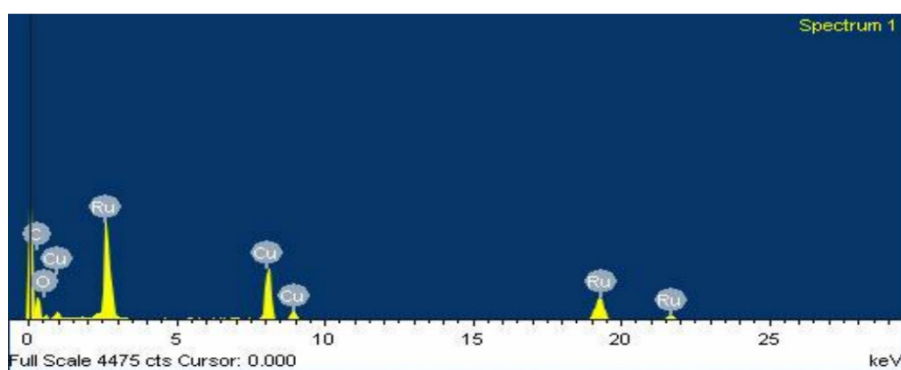


Fig. S2 EDX elemental analysis data of a single point inside HMRu NPs further confirms the totally removal of silica template.

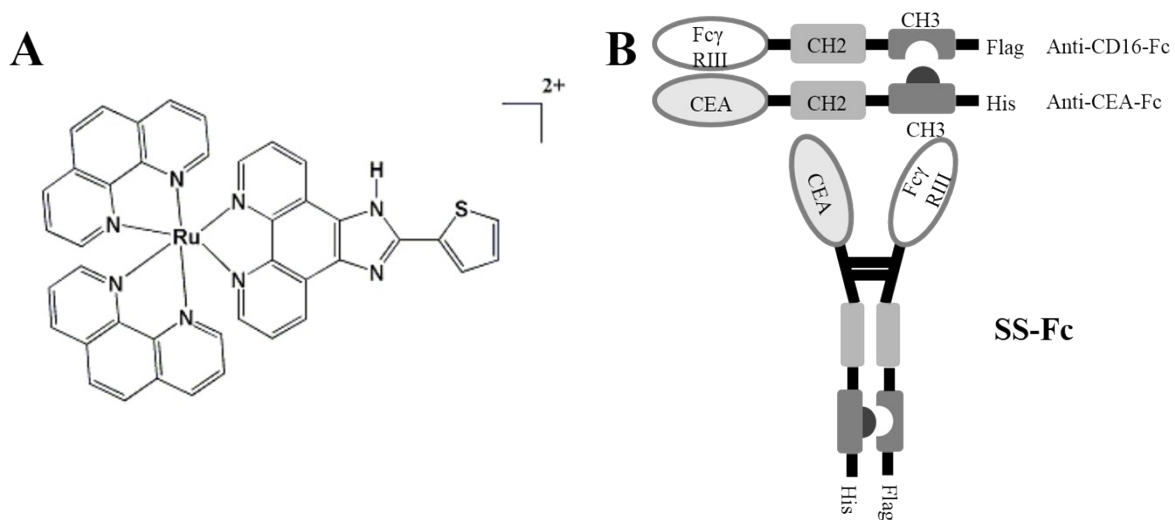


Fig. S3 (A) Schematic structures of RBT: $[\text{Ru}(\text{bpy})_2(\text{tip})]^{2+}$. (B) Schematic structures of SS-Fc bispecific antibody formed by heterodimerization of anti-CEA-Fc and anti-CD16-Fc mediated by a CH2–CH3 interaction.

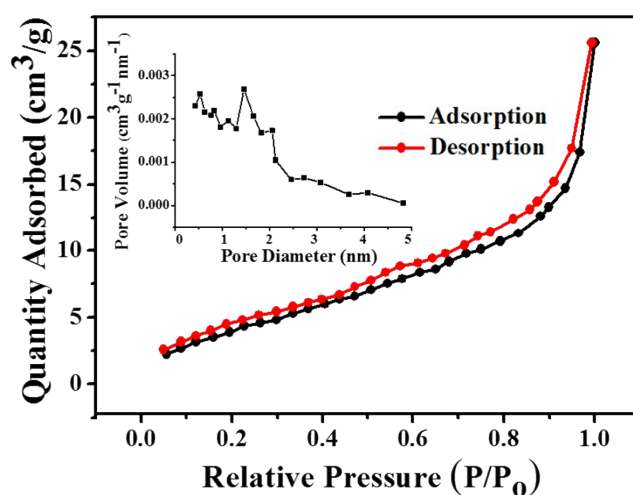


Fig. S4 N₂ adsorption/desorption isotherm and corresponding pore-size distribution curves (inset) of HMRu NPs after RBT loading (HMRu@RBT).

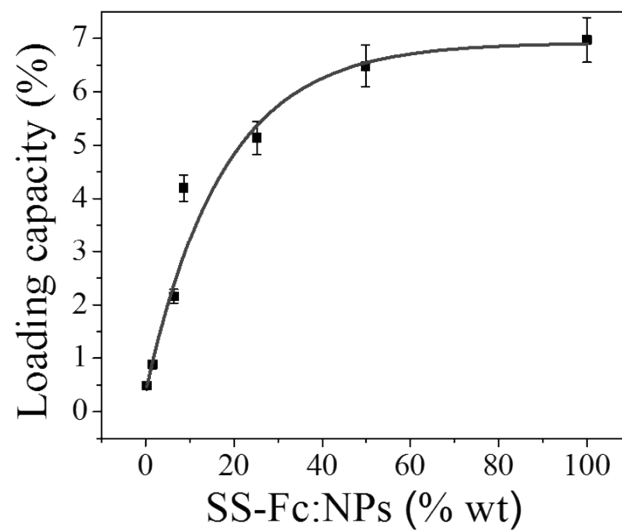


Fig. S5 Loading capacity of SS-Fc in HMRu@RBT at different weight ratio.

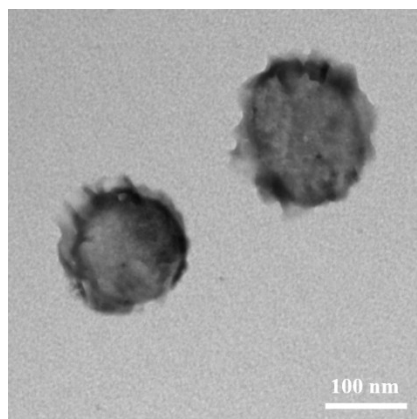


Fig. S6 Transmission electron microscopy (TEM) image of HMRu@RBT-SS-Fc. Scale bars, 100 nm.

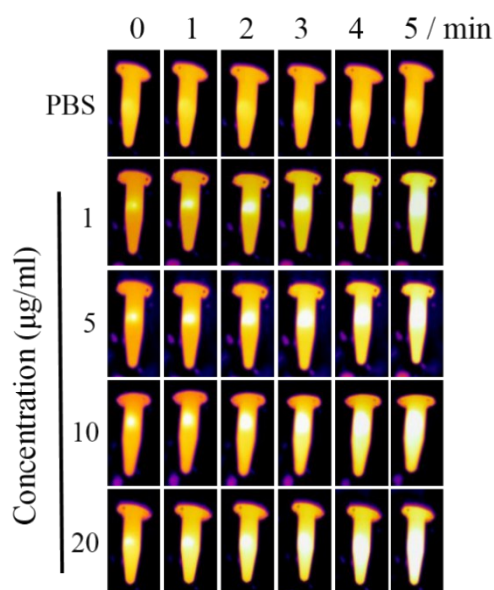
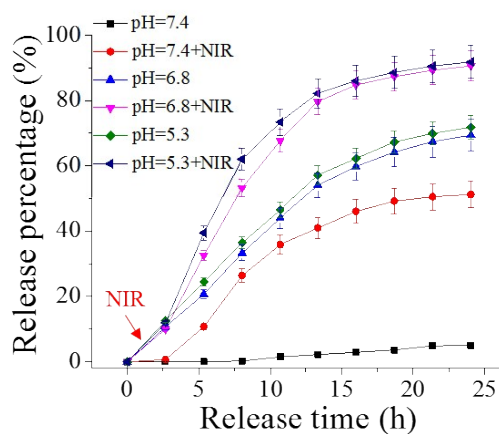


Fig. S7 IR thermal images of PBS, SS-Fc, HMRu, HMRu@RBT-SS-Fc solutions (20 µg/mL) under an 808 nm NIR laser at a power density of 300 mW cm⁻² for 5 min.



Release percentage	12 h	24 h
PBS (pH=7.4)	2.2 %	5.0 %
PBS (pH=7.4) +NIR	40.9 %	51.2 %
PBS (pH=6.8)	54.1 %	69.4 %
PBS (pH=6.8) +NIR	79.7 %	90.6 %
PBS (pH=5.3)	57.2 %	71.9 %
PBS (pH=5.3) +NIR	82.2 %	91.8 %

Fig. S8 *In vitro* acidic/NIR-sensitive release profiles of RBT from HMRu@RBT-SS-Fc with and without NIR laser irradiation in PBS of different pH values. Data are shown as mean ±S.D. (n = 3 independent experiments)

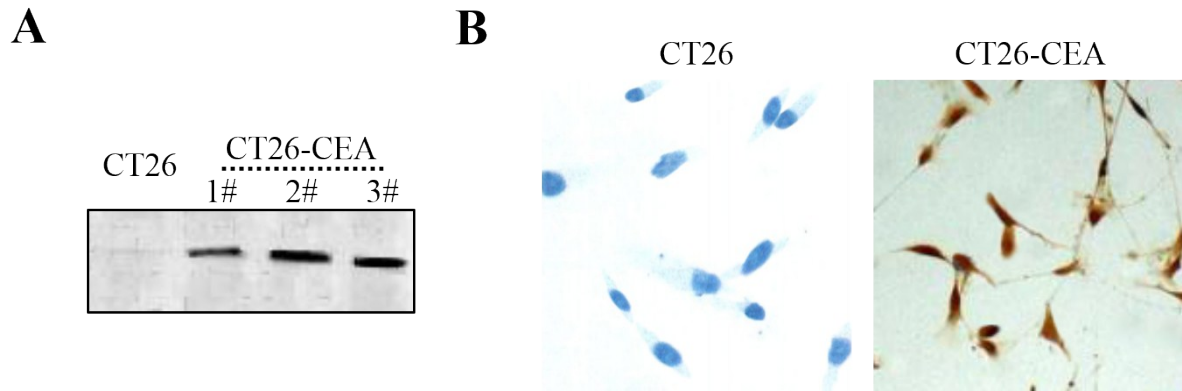


Fig. S9 (A) Expression of CEA in CT26 cell lines with and without lentiviral transduction. (B) Immunocytochemistry analysis of CEA-positive CT26 cells.

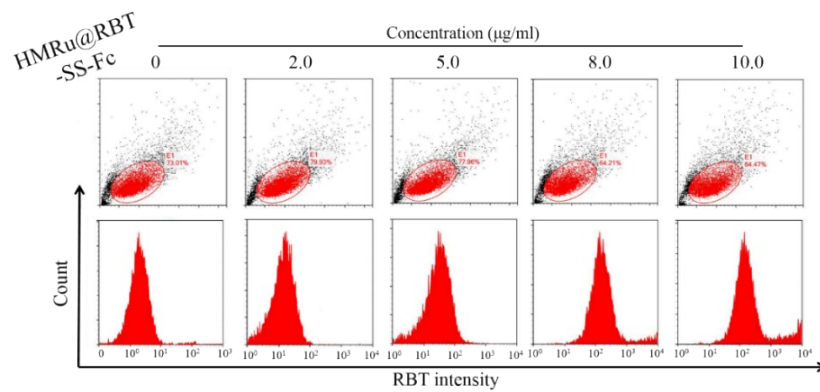


Fig. S10 Flow cytometric analysis of green fluorescent RBT in various concentrations of HMRu@RBT-SS-Fc.

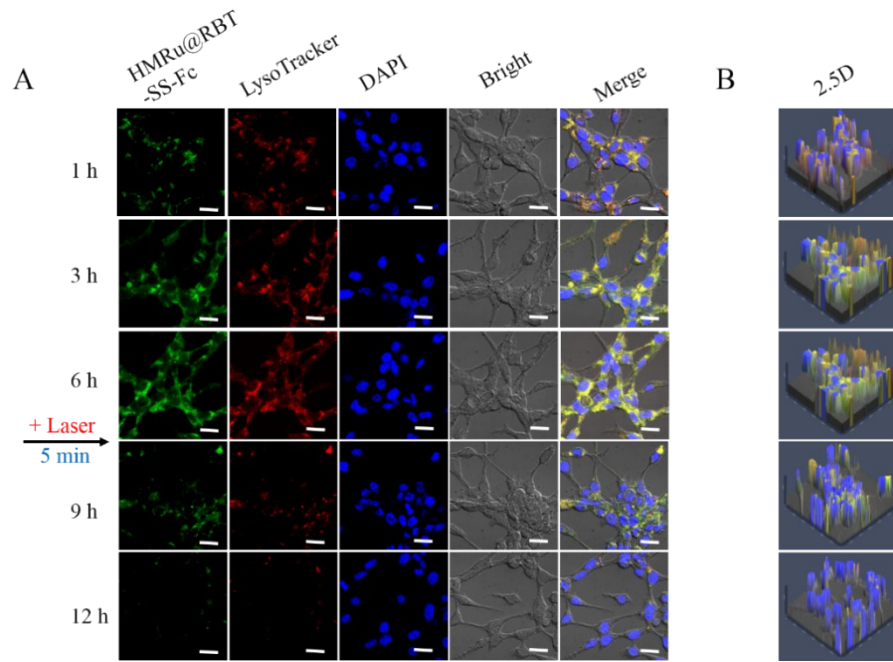


Fig. S11 (A) Time-dependent confocal microscopy of HMRu@RBT-SS-Fc successfully escaped from endosomes/ lysosomes. CT26-CEA cells were incubated with HMRu@RBT-SS-Fc (green) at pH=6.8 for 6 h and then irradiated by an 808 nm laser for 5 min to release RBT. Endo-lysosomes structure was labeled by LysoTracker in red; nuclei were labeled by DAPI in blue; scale bar: 20 μ m. (B) The 2.5D images show fluorescent intensity in the corresponding confocal microscopy images.

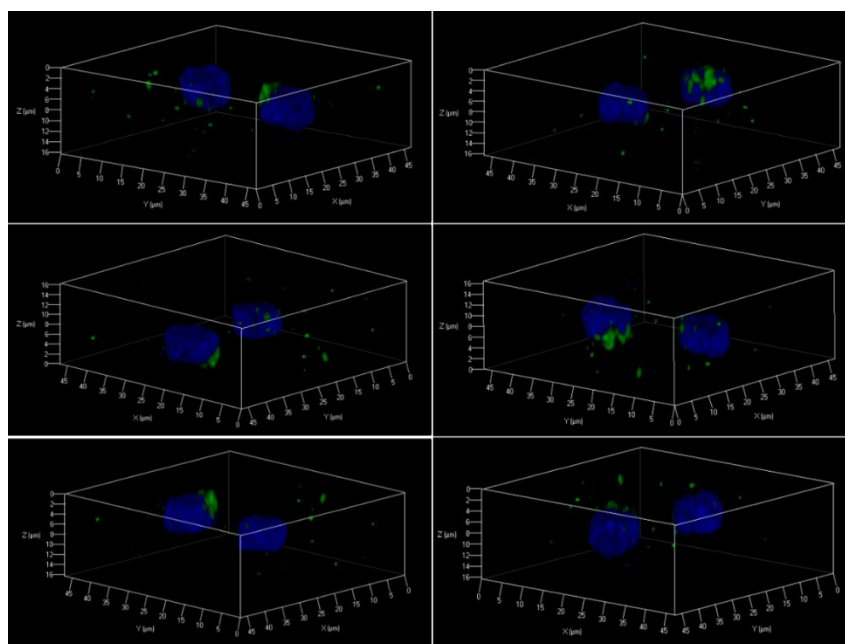


Fig. S12 3D images of NK cells binding with HMRu@RBT-SS-Fc observed from different angles by confocal microscopy. Green, NPs; Blue, NK cells.

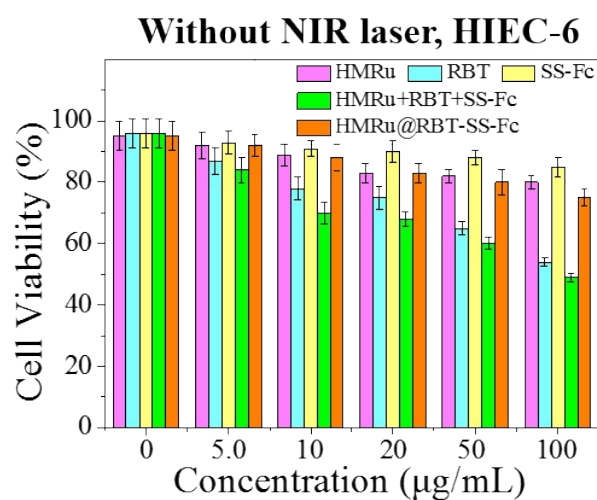


Fig. S13 Cell viabilities of HIEC-6 cells incubated with various concentrations of HMRu, RBT, SS-Fc, HMRu+RBT+SS-Fc and HMRu@RBT-SS-Fc without NIR laser irradiation. Data are shown as mean \pm S.D. (n = 3 independent experiments).

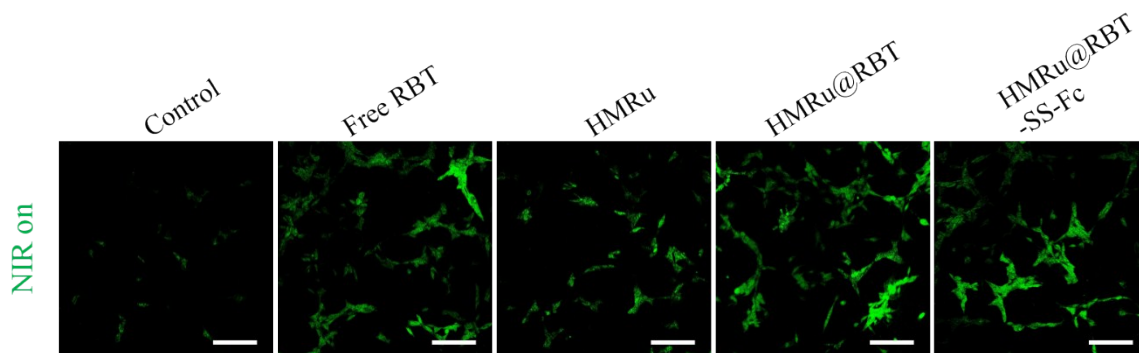


Fig. S14 ROS generation in CT26-CEA cells incubated with PBS, RBT, HMRu, HMRu@RBT and HMRu@RBT-SS-Fc. Cells were irradiated by an 808 nm NIR laser (300 mW cm^{-2} , 5 min). ROS was labeled with green fluorescent probes. Scale bar, 50 μm .

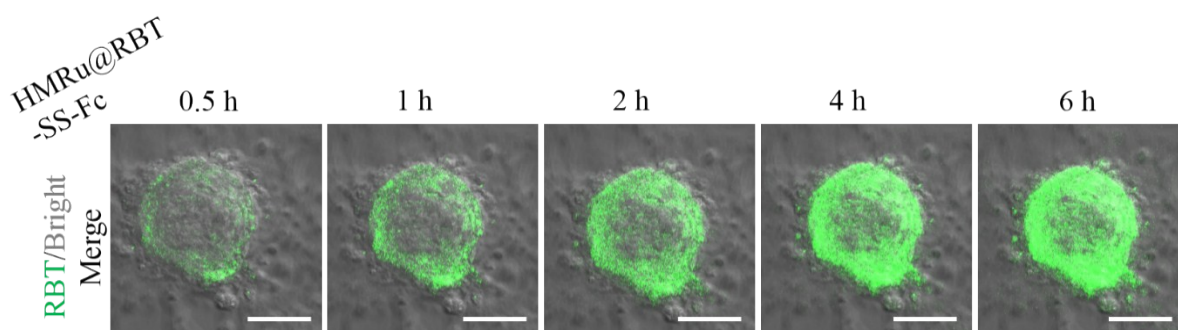


Fig. S15 Penetration of RBT into the 3D CT26-CEA tumor spheroid after incubation with HMRu@RBT-SS-Fc over time. CLSM images were obtained using the Z-stack scanning from the surface to the middle of the tumor spheroid at the fixed depth of 85 μm . Scale bar, 100 μm .

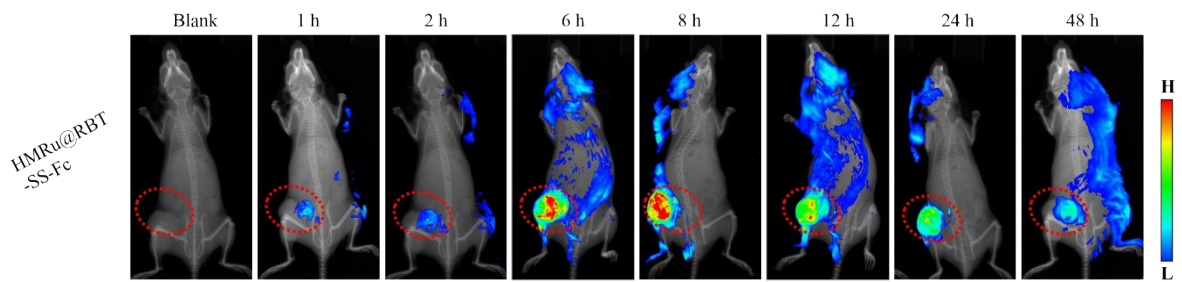


Fig. S16 *In vivo* fluorescence imaging of CT26-CEA tumor-bearing BALB/c mice after treatment of HMRu@RBT-SS-Fc for different time. Red circle: tumor site.

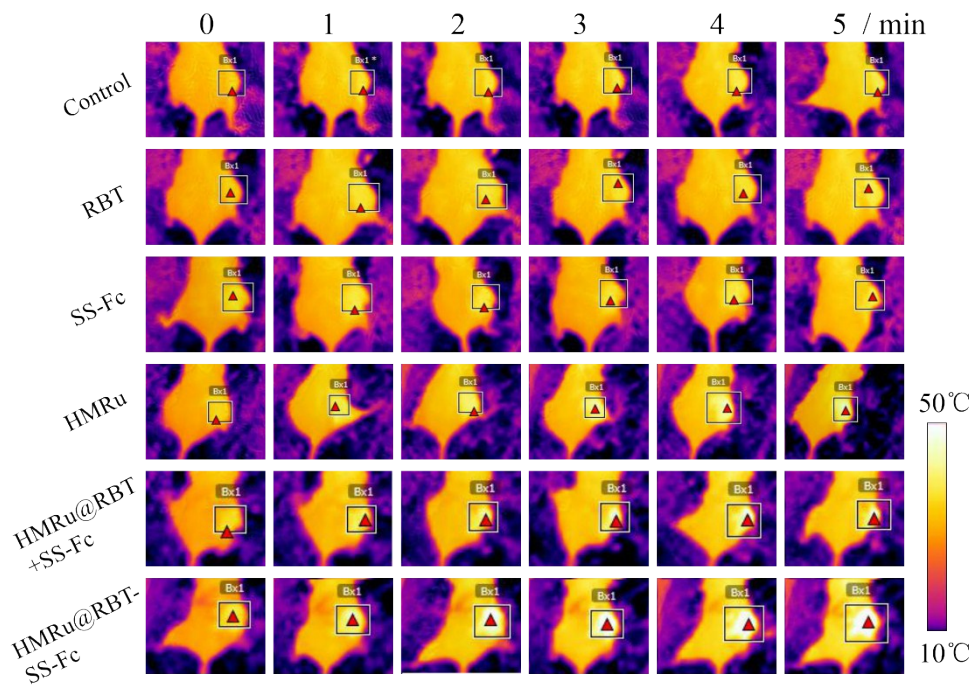


Fig. S17 IR thermal images of CT26-CEA tumor-bearing mice with injection of PBS, RBT, SS-Fc, HMRu, HMRu@RBT+SS-Fc, and HMRu@RBT-SS-Fc under the 808 nm NIR laser irradiation (300 mW cm^{-2}) for 5 min. Red triangle: maximum temperature.

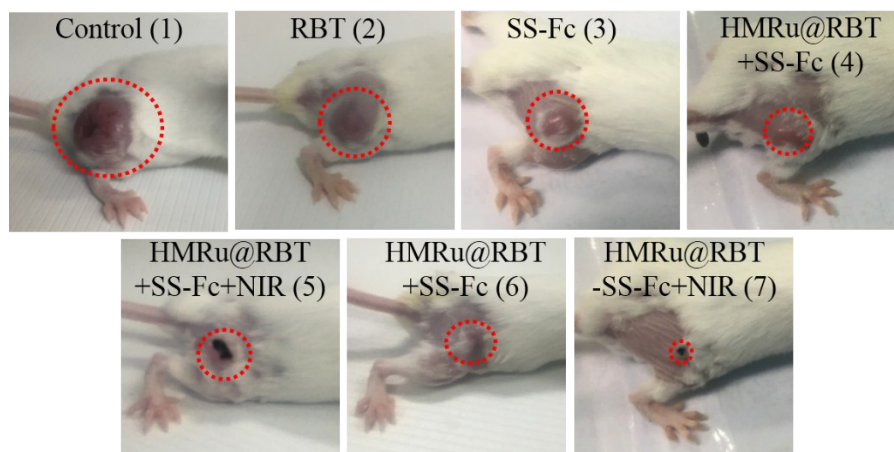


Fig. S18 Representative photographs of mice from different groups at 21 day after CT26-CEA tumor inoculation. Red circle: tumor site.

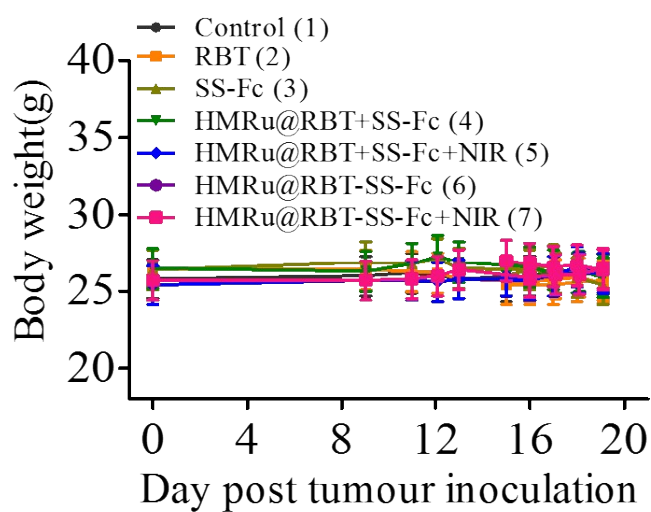


Fig. S19 Average body weight CT26-CEA tumor-bearing mice after different treatments.

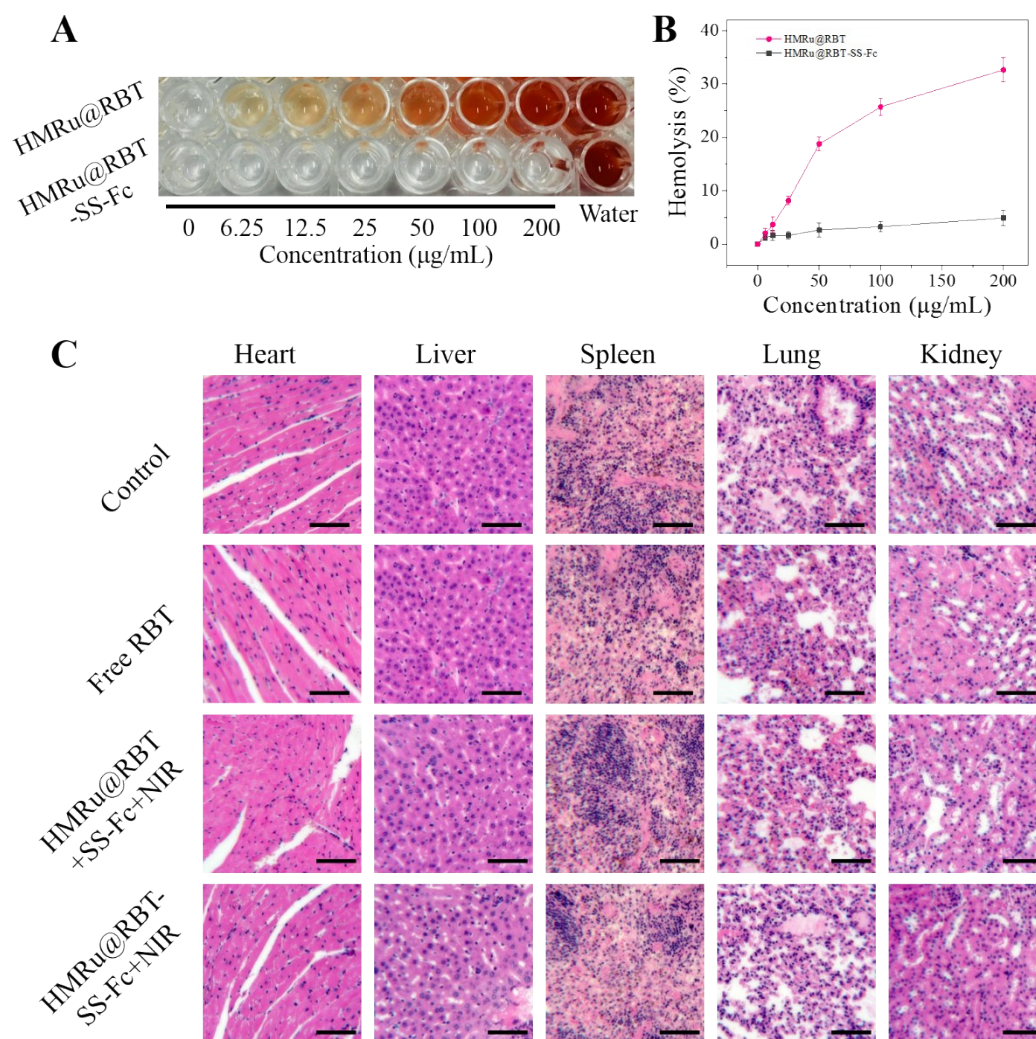


Fig. S20 (A) Digital images showing hemolysis of human red blood cells after incubation with various concentration of HMRu@RBT or HMRu@RBT-SS-Fc for 2 h at 37 °C. (B) Corresponding quantitative analysis of hemolysis of human red blood cells. (C) Pathological H&E stained images of tissue sections from major organs including heart, liver, spleen, lung and kidney of the BALB/c mice treated with PBS, Free RBT, HMRu@RBT+SS-Fc+NIR and HMRu@RBT-SS-Fc+NIR 21 days p.t.i. for *in vivo* biosafety evaluation. Scale bar, 50 μm .

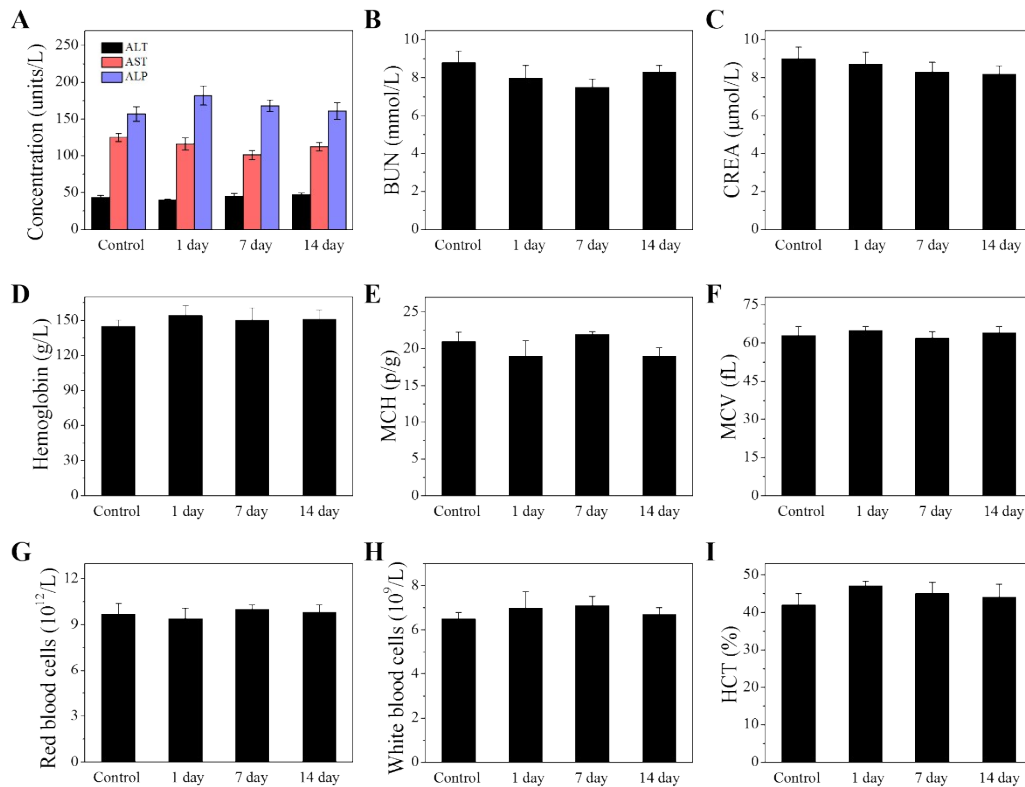


Fig. S21 Comparison of the blood biochemical parameters of BALB/c mice in 7 day, 13 day and 19 day post i.v. injection of HMRu@RBT-SS-Fc (5 mg kg^{-1}) and irradiation of the NIR laser (808 nm , 300 mW cm^{-2} , 5 min). A) The liver function related alanine aminotransferase (ALT), alkaline phosphatase (ALP), aspartate aminotransferase (AST). B) Nephric blood urea nitrogen (BUN) and C) creatinine (CREA) indicators showed no significant differences in comparison to the control, suggesting the negligible hepatotoxicity and nephrotoxicity of the HMRu@RBT-SS-Fc. D) Hemoglobin (HGB), E) mean corpuscular hemoglobin (MCH), F) mean corpuscular volume (MCV), G) red blood cell (RBC) counts, H) white blood cell (WBC) counts and I) hematocrit (HCT) levels of HMRu@RBT-SS-Fc with laser treated mice at different days. Number of independent BALB/c mice $n = 5$, mean \pm S.D.

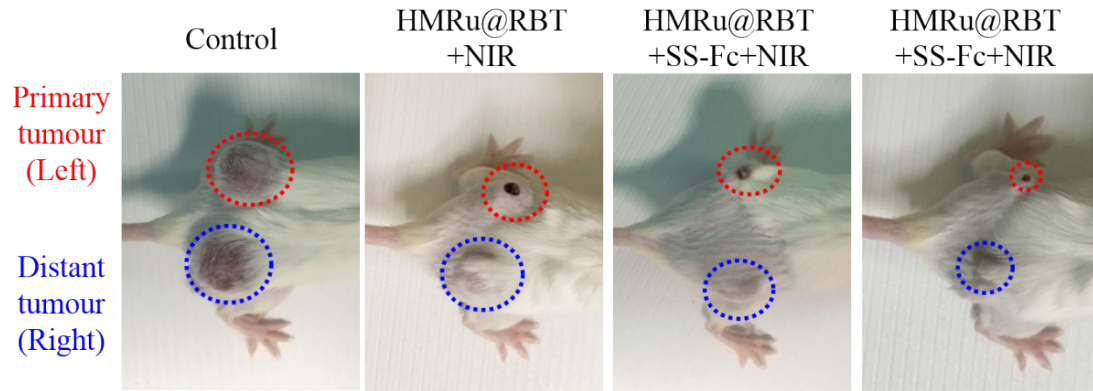


Fig. S22 Representative photographs of bilateral tumors-xenografted BALB/c mice three weeks after CT26-CEA cells inoculation. Mice were treated by intravenous injection of different nanoparticles, and only the left tumors were irradiated with the NIR laser (808 nm, 300 mW cm^{-2} , 5 min). Red circle: Primary tumor site; Blue circle: Distant tumor site.